JOURNAL OF MATERIALS SCIENCE **37** (2002) 1107–1113

Microstructure and environment-dependent fatigue crack propagation properties of Ti-48Al intermetallics

S. HAMADA, H. HAMADA, H. SUZUKI
Department of Mechanical Engineering, Sophia University, Japan
E-mail: h-suzuki@me.sophia.ac.jp

M. N. TAMIN
Faculty of Mechanical Engineering, Universiti Teknologi, Malaysia

A. NOZUE
Department of Mechanical Engineering, Sophia University, Japan

Fatigue crack propagation properties of Ti-48Al were studied by means of *in-situ* observation of the crack growth process under vacuum and air conditions. Three types of microstructures, namely, as-cast, duplex and fully lamellar structure were investigated in the present study. The results show that the crack growth behavior is dependent on the microstructure and the angle between the crack growth direction and orientation of lamellar colonies. The preferred path of crack propagation through the weakest phase of the structure associated with microcracking within the crack tip plastic zone has been investigated. The accelerated crack growth observed in air environment is attributed to absorption of air humidity at the crack tip plastic zone. This phenomenon is apparent through the observation of crack propagation process and the resulting fractured surface.

1. Introduction

Intermetallics based on γ-TiAl have been developed as high temperature structural materials because of their superior mechanical properties at high temperature and low density compared to conventional heat resistant alloys [1]. A lot of works report on the relationship between microstructure and mechanical properties, especially on fatigue and fracture behavior [2–4]. The microstructure of the material can be controlled by thermo-mechanical or heat treatment in order to obtain preferred microstructures for specific applications [5–7]. Typical microstructures of γ-TiAl based alloys can be classified into three types [1]: two phase lamellar structure which consists of thin α_2 (Ti_3Al) and γ lamellae, two phase duplex structure consisting of equiaxed γ grains and lamellar colonies, and monolithic γ structure in single phase alloys. It has been reported [1] that fine grained duplex structure exhibits improved strength and ductility, whereas the lamellar structure possesses excellent creep resistance and fatigue properties. The fatigue and fracture properties of the material are strongly dependent on the orientation of the lamellar colonies and the direction of crack propagation [2, 3]. This specific behavior has been observed during fatigue tests [2] and by *in-situ* observation of crack propagation [8]. In the present study the fatigue crack growth in typical microstructures of TiAl intermetallics was examined in detail by means of *in-situ* observation of crack extension in vacuum and air conditions. The microstructure related crack propagation behavior obtained by fatigue tests is shown in the crack propagation rate da/dN versus stress intensity factor ΔK range plots. The effects of crack closure and environment on the crack propagation behavior are also discussed.

2. Experimental procedure

2.1. Material and specimen preparation

The Ti-48Al alloy used in this study is supplied by Mitsubishi Material Corporation. The chemical composition of the material is shown in Table I. The specimens are cut from the as-cast ingot and heat treated in argon gas atmosphere. The time-temperature profiles are chosen with the aid of the Ti-Al phase diagram [9] and several published reports on microstructure and heat treatment of Ti-Al intermetallics [1, 5, 7] in order to obtain samples possessing fully lamellar and duplex microstructures. The fully lamellar structure is obtained by heat treatment of the sample at 1668 K for 80 minutes followed by furnace cooling to room temperature. The duplex structure is obtained by a heat treatment at 1543 K for 120 minutes and furnace cooling to room temperature. We call as received material "as-cast", and the material having fully lamellar and duplex structure "fully lamellar" and "duplex" throughout the paper.

TABLE I Chemical composition of Ti-48Al intermetallics

Element	Al	C	H	N	O	Ti
wt%	34.48	0.006	0.001	0.005	0.08	balance
at.%	48.3	–	–	–	–	balance

2.2. Fatigue test

Fatigue crack growth and fracture toughness tests are performed on compact tension (CT) specimens. The geometry of the specimens follow the ASTM E399-90 specification with a specimen width of $W = 35$ mm and a thickness of $B = 6$ mm. The CT specimens are machined from the as-cast ingot so that the load axis of the specimen is normal to the radial direction of the ingot.

3. Experiment

3.1. Microstructure

The three types of microstructure, namely, as-cast, fully lamellar and duplex structure are examined in the present study. The microstructure of the as-cast material consists of equiaxed lamellar grains (200 to 300 μm in diameter) and a small amount of γ grains (120 to 200 μm in diameter). The duplex structure consists of large lamellar grains (1000 to 4000 μm in diameter) and equiaxed γ grains (200 to 300 μm in diameter). The volume ratio of lamellar to γ grains in the duplex structure has been estimated to 7 : 3. The fully lamellar structure consists of lamellar grains with nominal diameter of 400 to 700 μm. The size of the lamellar grains is larger in the fully lamellar structure material than in the as-cast material. In addition, no γ grains are observed in the fully lamellar structure.

3.2. Mechanical properties

The mechanical properties of each microstructure of the Ti-48Al alloy are summarized in Table II. Tensile tests are conducted using specimens with a gage length of 18.8 mm and a cross section of 2.5 mm × 4 mm. The specimens are machined from the as-cast ingot so that the longitudinal axis of the samples is parallel to the circumferential direction of the ingot.

The fracture toughness tests are performed as specified in the ASTM E399-90 document. In the present study, the fracture toughness is not determined according to the plane strain condition because of the relatively small thickness of the specimen. Therefore, the fracture toughness K_Q is determined to compare the results of the materials with various microstructures.

Vickers' hardness values of lamellar and γ grains in each of the three different microstructures are measured using a micro-vickers hardness tester with an applied load of 4.9 N.

TABLE II Mechanical properties of Ti-48Al intermetallics of three typical microstructures

		As Cast	Duplex	Fully lamellar
Tensile strength	MPa	380	290	190
Plastic elongation	%	0.4	0.4	0.3
K_{max}	MPa · m$^{1/2}$	18.6	21.0	20.5
K_Q	MPa · m$^{1/2}$	14.6	19.0	17.6
Hardness				
Lamellar grain	$HV_{0.5}$	320	270	290
γ grain	$HV_{0.5}$	270	180	–
Grain size				
Lamellar grain	μm	200–300	1000–4000	400–700
γ grain	μm	120–200	200–300	–

3.3. *In-situ* observation of crack growth in vacuum condition

Fatigue crack growth test in vacuum condition is carried out using a Shimadzu electro-hydraulic testing machine fitted with a scanning electron microscope. This set-up enables *in-situ* observation of the crack growth process. A vacuum of 10^{-3} Pa is established throughout the test. A sinusoidal load with a stress ratio (R) of minimum to maximum load of 0.1 and a frequency of 20 Hz is applied to the specimen. A higher stress ratio of $R = 0.5$ is utilized to examine the effect of crack closure on crack propagation behavior. In addition to the *in-situ* observation of the crack growth process, crack lengths, a, were recorded at prescribed interval of load cycles, N, and the resulting data is analyzed to obtain the crack propagation rate, da/dN. The corresponding applied stress intensity factor range, ΔK, is determined from the value of the applied load amplitude and the measured crack length.

3.3.1. Crack growth in lamellar structure

Both as-cast and fully lamellar structures are composed primarily of lamellar structure. The angle between the direction of crack growth and the orientation of lamellar layer is known to strongly affect the crack propagation behavior [2, 3]. Fig. 1 shows an example of the crack growth process in vacuum condition, as observed in the fully lamellar structure. The load axis corresponds to the vertical direction of the micrographs in Figs 1 through 5. The micrographs shown in Fig. 1 are taken at every 1200 fatigue cycles under a stress intensity factor range of 14.5 MPa · m$^{1/2}$ and a stress ratio, $R = 0.1$. In this figure, the angle between the orientation of the lamellar layers and the direction of main crack propagation is less than 45 degrees, resulting in translamellar fracture. We call this case (<45 degrees) "sharp angle" and the opposite case (>45 degrees) "blunt angle" in this paper. From these observations, the crack growth process can be described as follows:

The crack extends along α_2/γ interface of the lamellar structure (Fig. 1a), where the cohesive force is expected to be low. The crack is deflected and grew across the γ layer. Crack retardation occurred at the next interface of phases that exists in the lamellar structure (Fig. 1b) followed by initiation of microcracks in the vicinity of the main crack tip (Fig. 1c). This microcrack is initiated within the plastic zone associated with the crack tip, which is estimated to be 170 μm in size. The size of the plastic zone at the tip of the fatigue crack is calculated from macroscopic yield strength shown in Section 3.2 and the value of applied load under the assumption of plane-stress condition. With additional

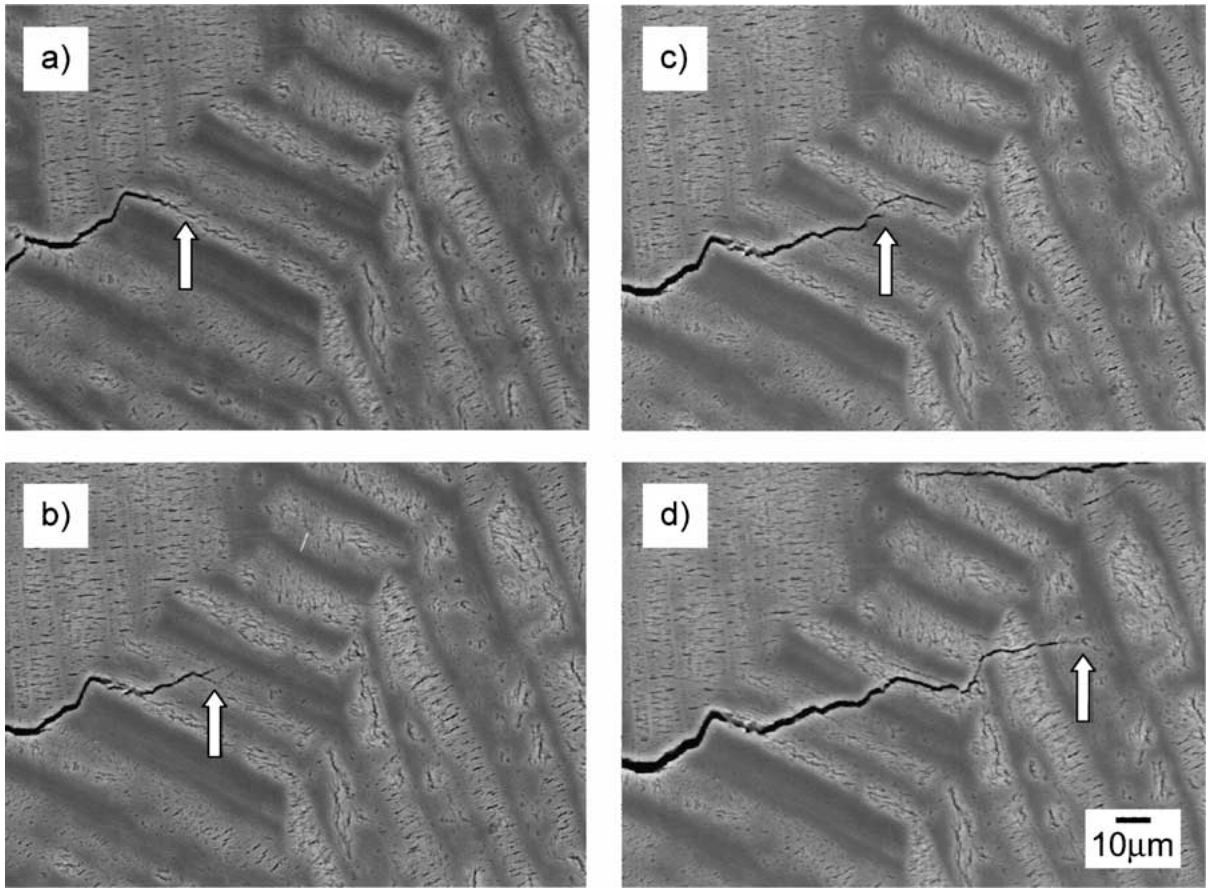

Figure 1 Crack growth process in lamellar structure where the direction of crack propagation and the lamellae forms a sharp (<45 degrees) angle. The stress intensity factor range is 14.5 MPa $\cdot$ m$^{1/2}$ and the stress ratio is 0.1. Photographs are taken every 1200 cycles of fatigue. The arrow in each figure indicates the tip of the main crack. The load axis corresponds to the vertical direction of the figure.

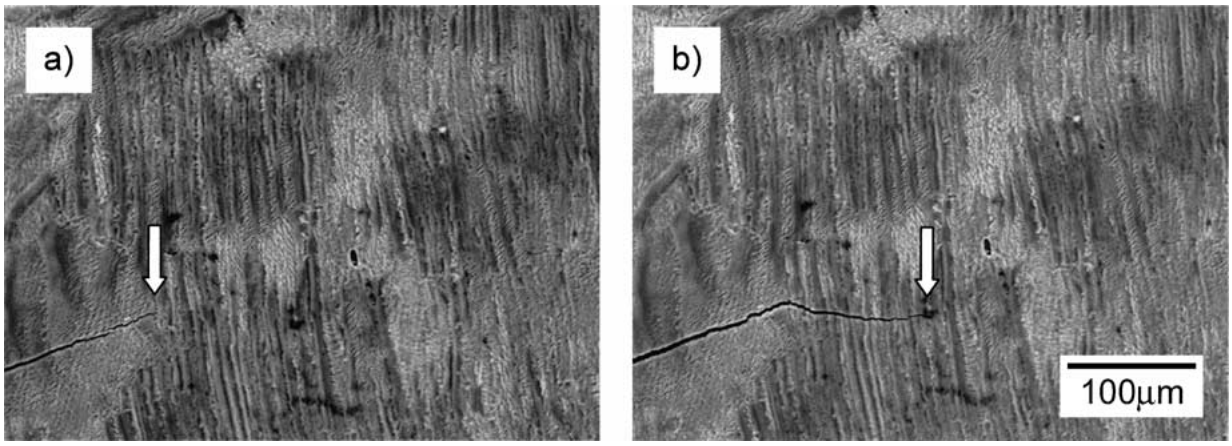

Figure 2 Crack growth in the lamellar structure where the directions of the crack propagation and the lamellae forms a blunt (>45 degrees) angle. The stress intensity factor range is 16.0 MPa $\cdot$ m$^{1/2}$ and the stress ratio is 0.1. Fig. 2b is taken 6000 fatigue cycles of fatigue after Fig. 2a. The arrow in each figure indicates the tip of the main crack.

load cycles, the main crack extends and joins the microcrack and the process continues when the crack tip reaches the next neighboring lamellar grains.

When the direction of the main crack propagation and the orientation of lamellar layer forms blunt angle, crack growth is likely to be retarded between layers of lamellar structure. With additional fatigue cycles, the crack is deflected to extend across lamellar layers. An example of this translamellar crack growth behavior is shown in Fig. 2 for as-cast material at an applied stress intensity factor range of 16.0 MPa $\cdot$ m$^{1/2}$ and stress ratio, $R = 0.1$.

3.3.2. Crack growth in duplex structure

An example of crack growth in duplex structure is shown in Fig. 3. These micrographs are taken at every 200 fatigue cycles. The applied stress intensity factor range is 16.5 MPa $\cdot$ m$^{1/2}$ and stress ratio, $R = 0.1$. The crack propagation process within γ grains in the duplex structure can be described as follows:

The main crack propagates along γ/lamellar grain boundary of low resistance to crack growth (Fig. 3a). The crack propagation is retarded forming a zigzag profile of the crack extension. Simultaneously, a microcrack is initiated at γ/lamellar grain boundary and

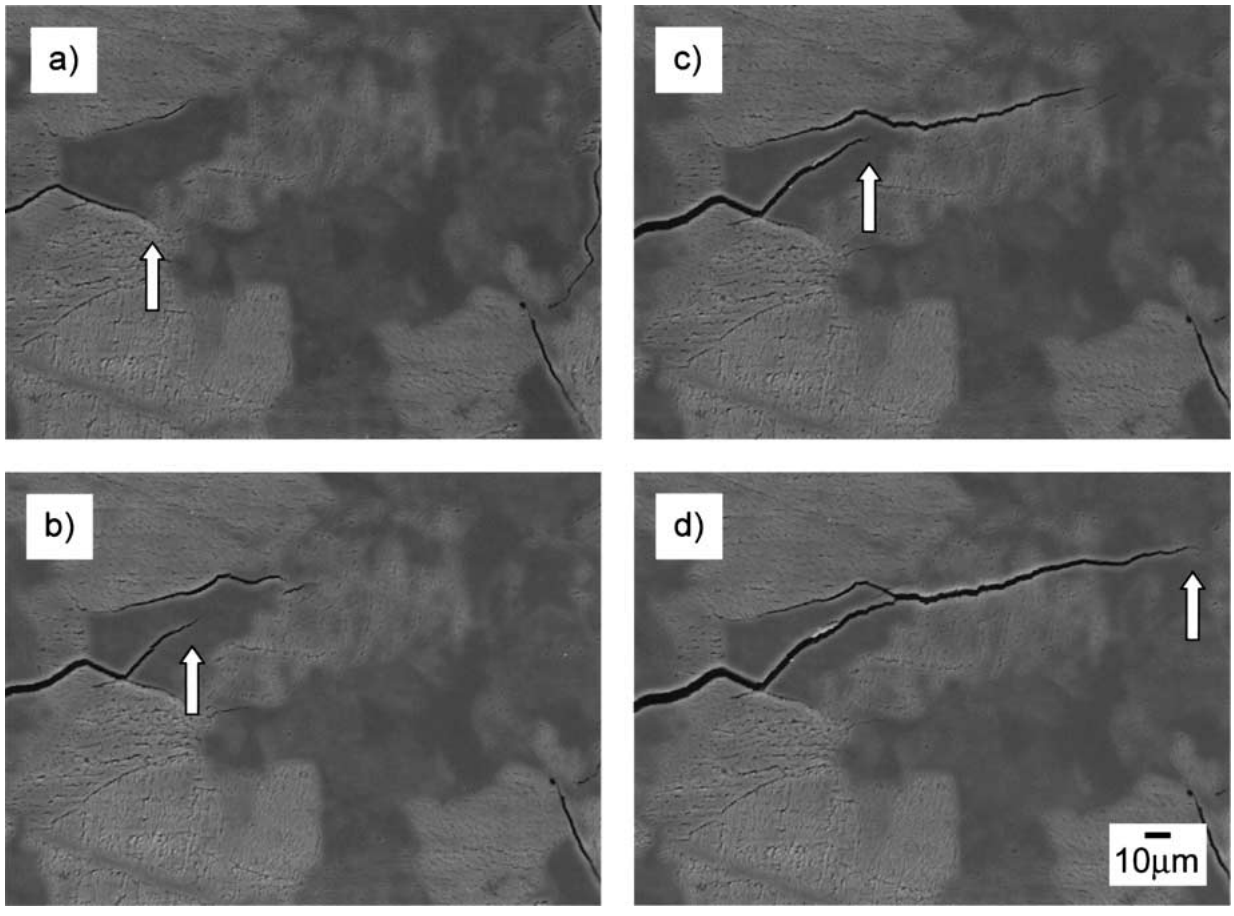

Figure 3 Crack growth in duplex structure illustrating crack extension in γ grains. Stress intensity factor range is 16.5 MPa $\cdot$ m$^{1/2}$ and the stress ratio is 0.1. Photographs are taken every 200 cycles of fatigue. The arrow in each figure indicates the tip of the main crack.

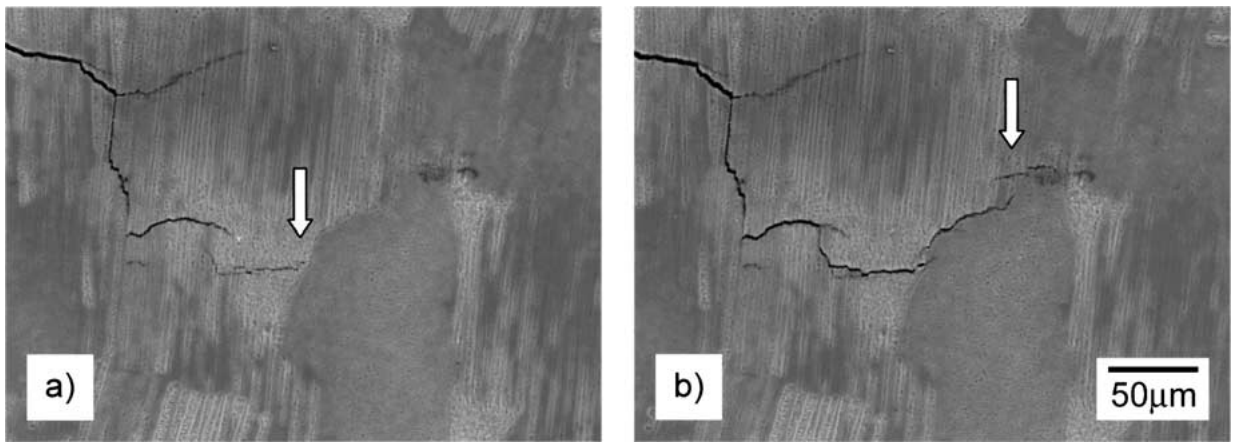

Figure 4 Crack growth in duplex structure when the crack propagates along γ grain boundary. Stress intensity factor range is 13.0 MPa $\cdot$ m$^{1/2}$ and the stress ratio is 0.1. Fig. 4b is taken 80000 cycles of fatigue after Fig. 4a. The arrow in each figure indicates the tip of the main crack.

grows under the Mode I crack driving force (Fig. 3b). With additional load cycles, the main crack propagates into the γ phase forming a shear ligament that connects with the microcrack. This leads to rapid crack extension (Fig. 3c and d).

The main crack that propagates along the γ grain boundary tends to halt when the crack encounters a material phase with higher crack growth resistance such as lamellar layers oriented perpendicular to the crack growth direction. In such a case, the crack extends with many microcracks initiated at boundaries of γ and lamellar grain, particularly in the crack tip region. An example of the crack growth process is shown in Fig. 4 which occurred at a stress intensity factor range of 13.0 MPa $\cdot$ m$^{1/2}$ and load ratio, $R = 0.1$. The size of a typical crack tip plastic zone is estimated to be about 70 to 75 μm. In Fig. 4a, crack extension is retarded when the tip reaches the γ grain boundary. An additional 80000 fatigue cycles resulted in several microcracks appearing at the α_2/γ grain boundary ahead of main crack. These microcracks contribute to relaxation of stress that decreases the crack tip driving force leading to crack growth deceleration.

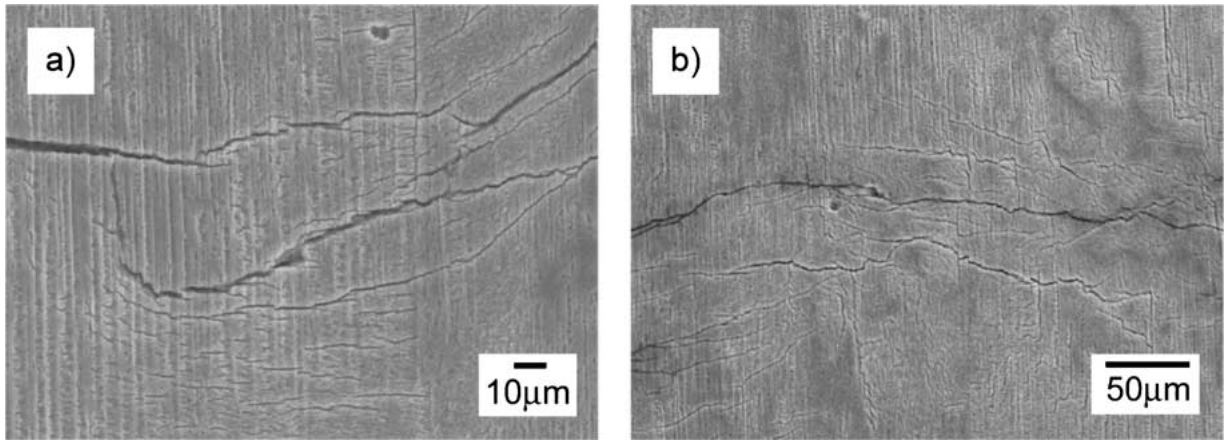

Figure 5 Examples of fatigue crack propagation in air conditions. (a) is as-cast material, stress intensity factor range is 11.0 MPa · $m^{1/2}$, and stress ratio is 0.1. (b) is duplex structure, stress intensity factor range is 5.0 MPa · $m^{1/2}$, and the stress ratio is 0.5. Both cases show many microcracks initiated around the main crack.

3.4. Crack growth in air condition

Fatigue crack growth tests are conducted in laboratory air to determine the crack growth response and assess the effect of environment on the crack propagation property. An electrohydraulic testing machine (MTS Corporation) is used in the experiment. The specimen is fatigued at a loading frequency of 20 Hz. Crack length measurements are taken with the aid of an optical traveling video scope.

It was observed that many parallel microcracks are initiated on both sides of the main crack, as shown in Fig. 5. This cracking feature with large number of microcracks is observed only in specimen fatigued in air condition and at low stress intensity factor range. However, the feature prevails in all microstructures of the Ti-48Al alloy examined in the present study.

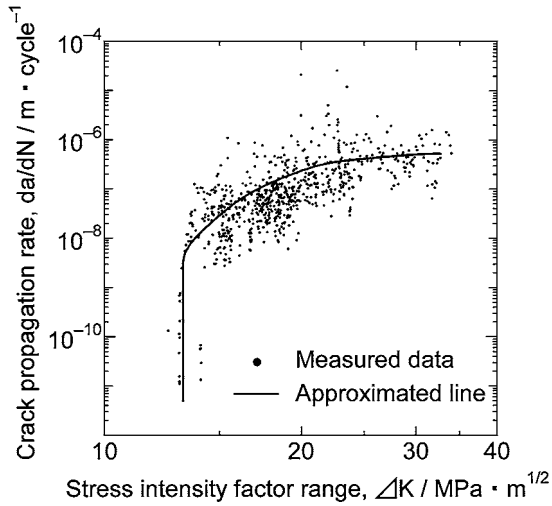

Figure 6 Crack propagation rate vs. stress intensity factor range are presenting measured and approximated crack propagation property of Ti-48Al intermetallic. The dots are indicating the measured values. Solid line is an approximated line obtained from measured data. The data are obtained from the as-cast material in vacuum with the stress ratio 0.1.

4. Discussion

The observed crack propagation behavior of the cast Ti-48Al alloy is expressed in terms of crack propagation rate, da/dN, versus stress intensity factor range, ΔK, diagram. The crack propagation rate for the as-cast material in vacuum condition at $R = 0.1$ is shown in Fig. 6. Crack propagation process in the as-cast structure occurs by initiation and growth of microcracks ahead of the main crack tip resulting in crack growth acceleration and deceleration, as described in previous section. Consequently, a large scatter of data occurs in the intermediate crack growth region. An approximated trend line is obtained by the least squares fitting method, shown as a solid line in Fig. 6, to represent the nominal behavior of the crack. This nominal crack propagation property will be utilized in comparing and discussing crack propagation response in the different types of microstructure.

4.1. Microstructure and crack growth in lamellar structure

Crack propagation in lamellar structure is strongly affected by the angle between the direction of crack propagation and the orientation of lamellar layer, as illustrated in Figs 1 and 2. *In-situ* measurements of crack growth rate, da/dN, and the corresponding stress intensity factor range, ΔK, are sorted according to the angle and morphology of the fracture surface for each type of microstructure. Schematic of the sorting conditions is illustrated in Fig. 7. The sorted crack growth types for the as-cast material (Fig. 6) is shown in Fig. 8. Results show that the number of occurrences for the blunt angle and inter-layer (case c in Fig. 7) is the smallest, indicating that this type of crack growth is least possible showing the dependence of crack growth to microstructure and morphology. Other types of crack growth, as defined in Fig. 7, occur with almost equal possibility. The results also indicate that fatigue crack propagates faster between layers of lamellar structure (inter-layer) than across the layers (trans-layer) for both cases of sharp and blunt angles. When the angle is sharp, the crack propagates between layers of lamellar structure where the interface of different (α_2/γ) or the same (γ/γ) kind of phase exist, thus the force to break the bond between phases is expected to be small. On the other hand, when the angle is blunt, the crack tends to stop between layers of lamellar causing blunting of the crack and simultaneous initiation of microcracks (see Fig. 2).

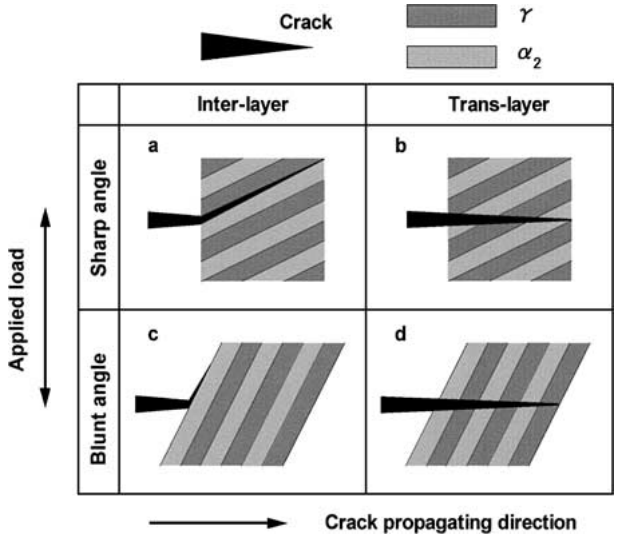

Figure 7 Schematic representation of conditions used to sort results of crack growth measurement in lamellar structure.

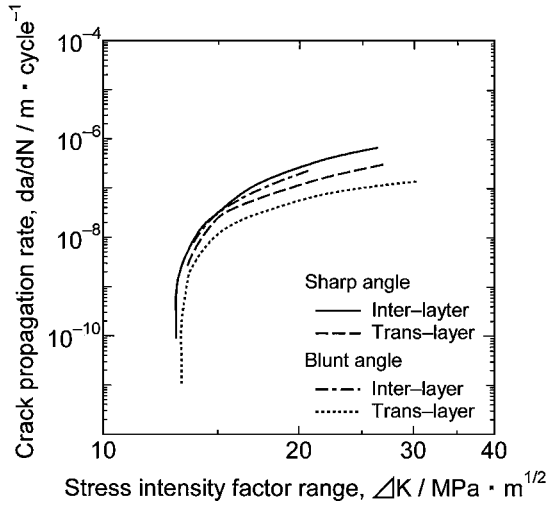

Figure 8 Property of crack propagation in lamellar structure. Observed properties are sorted according to the angle between the direction of fatigue crack and the orientation of lamellar layer, in addition to the mode of crack growth of inter-layer and trans-layer of lamellar structure. Experiments are conducted in vacuum condition with stress ratio 0.1.

The good correlation of the *in-situ* observation of crack growth process and the measured crack growth rate behavior ($\mathrm{d}a/\mathrm{d}N - \Delta K$ plot) suggests that fatigue crack propagates selectively through path of weakest bond in the structure. Otherwise, the crack growth is retarded and stopped to consume energy from the crack tip driving force.

4.2. Effect of environment on crack growth

The crack growth rate response for the three microstructures of Ti-48Al alloy in vacuum and air is compared in Fig. 9. Results show that the crack growth rate for the alloy is higher in air environment regardless of the type of microstructure. In addition, similar effect of environment holds for both conditions of stress ratios, $R = 0.1$ and 0.5. It is worth noting in Fig. 9 that the results of the test for stress ratio, $R = 0.5$, may demonstrates crack growth deceleration that could be due to crack closure effect.

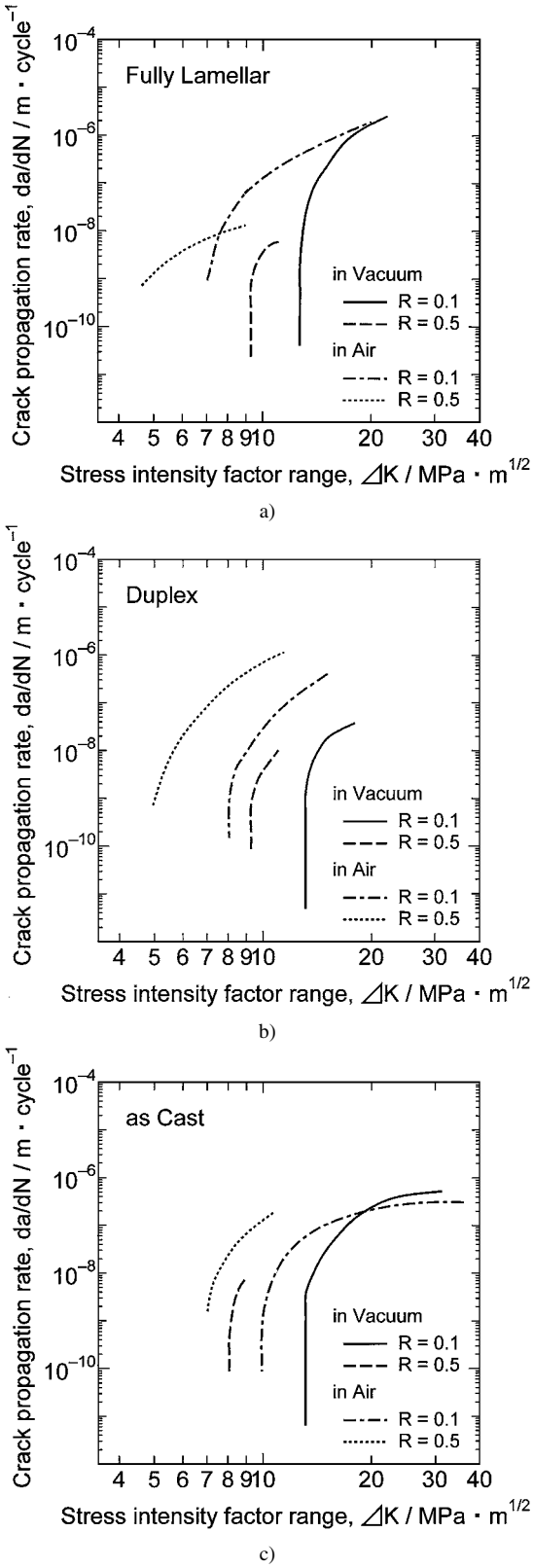

Figure 9 Property of crack propagation in vacuum and air for three types of microstructures, (a) fully lamellar, (b) duplex, and (c) as-cast.

This environmental effect is caused by absorption of humidity from the atmosphere through the surface of the specimen and subsequent reaction with aluminum element in the plastic zone at the tip of the crack [10–12]. Fig. 10 compares fracture surfaces of fully lamellar structure specimen tested in air condition at locations near the free surface with that in the bulk region of the fracture plane. Fracture surface near the

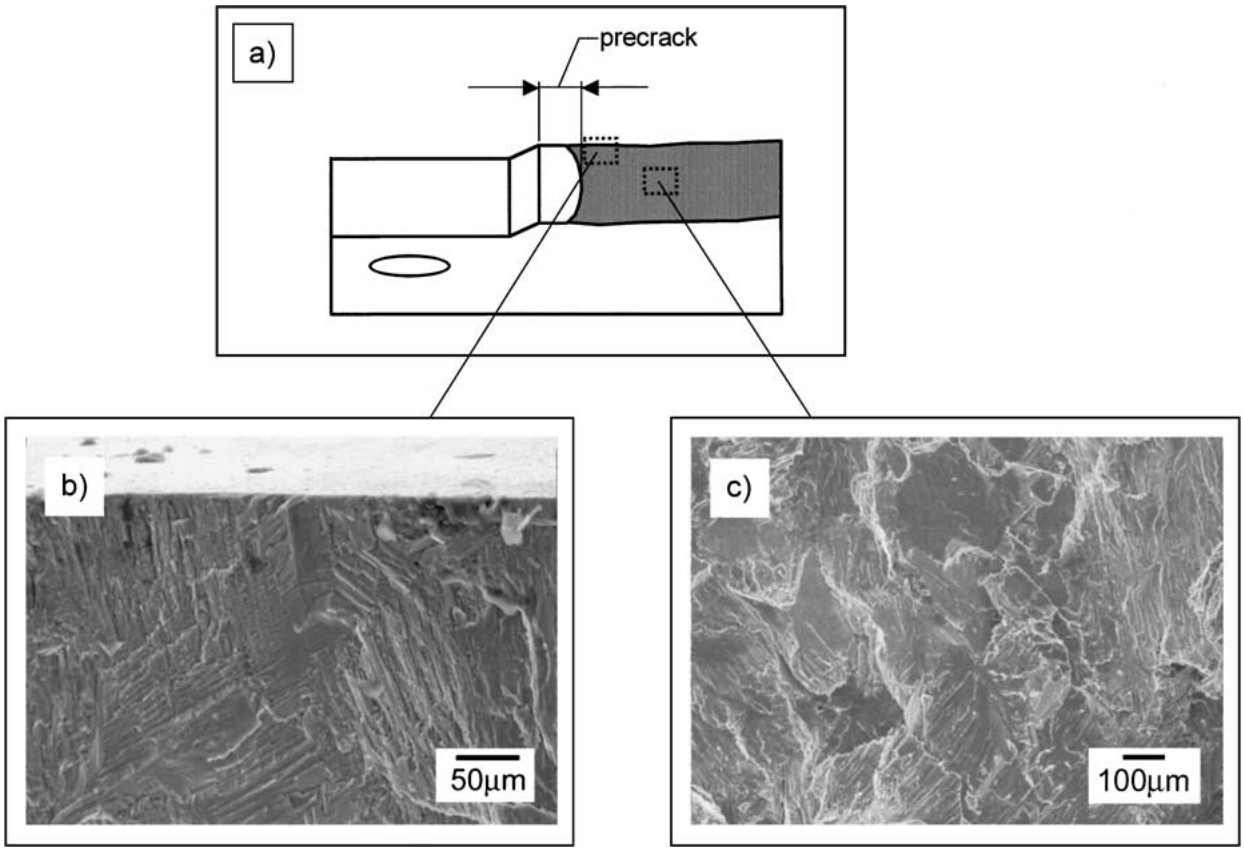

Figure 10 Fracture surface of a compact tension specimen of fully lamellar structure tested in air comparing the difference in the morphology depending on the regarded area of the sample. The stress ratio is 0.5. (a) shows a schematic drawing of fractured specimen exhibiting the approximate positions of (b) surface of the specimen and (c) bulk of the specimen. Note that many fine parallel lines independent of lamellar structure are present in (b).

edge of the specimen shows fine parallel lines that are independent of lamellar grains orientation. These are not observed at the bulk region of the specimen. This indicates that the fine lines correspond to microcracks observed in Fig. 5. In addition, the effect of environment diminishes at high stress intensity factor range, as illustrated in Fig. 9. At high level of stress intensity factor range, the crack propagates at a fast rate. As a result, insufficient time is allocated for absorption of air humidity towards the crack tip, thus minimizes environmental embrittlement.

5. Conclusion

Fatigue crack propagation behavior of Ti-48Al intermetallics is studied by *in-situ* observation of crack growth process under vacuum and air conditions. Three representative microstructures, namely, as-cast, fully lamellar and duplex structure of the TiAl intermetallics are used in the present study. Measurements of fatigue crack extension are correlated with types of microstructure. The effect of environment on the resulting crack growth behavior is examined. The results can be summarized as follows:

(1) Crack propagation is strongly affected by microstructure and the angle between crack propagation direction and the orientation of lamellar colony.

(2) The observed crack growth response is classified into possible modes of crack propagation including inter-layer and trans-layer. The preferred path of crack propagation in lamellar structure has been established; it goes through the weakest bond of the interface of different (α_2/γ) or the same (γ/γ) kind of phases with associated microcracking within the plastic zone around the tip of the crack.

(3) Crack growth is accelerated in air condition. This phenomenon is attributed to the effect of absorption of air humidity to the crack tip plastic zone. This environmental effect is apparent through the observation of crack propagation and the resulting fracture surface.

References

1. Y. W. KIM, *JOM* **14** (1989) 24.
2. R. GANAMOORTHY, Y. MUTOH, K. HAYASHI and Y. MIZUHARA, *Scripta Metall.* **33** (1995) 909.
3. S. MITAO, T. ISAWA and S. TSUYAMA, *ibid.* **26** (1992) 1405.
4. M. CHEN, D. LIN and D. CHEN, *ibid.* **36** (1997) 497.
5. B. D. WORTH, J. M. LARSEN, S. J. BALSONE and J. W. JONES, *Metall. Materials Trans.* **28A** (1997) 825.
6. Y.-W. KIM, *Acta Metall. Mater.* **40** (1992) 1121.
7. T. KUMAGAI, E. ABE, M. TAKEYAMA and M. NAKAMURA, *Scripta Metall.* **36** (1997) 523.
8. K. W. CHAN and D. S. SHIH, *Metall. Materials Trans.* **28A** (1997) 79.
9. J. L. MURRAY, in "Binary Alloy Phase Diagram," edited by T. B. Massalski (ASM, Material Park, OH, 1986) p. 173.
10. H. GILBERT, M. CATHERRINE, T. ANNE and P. JEAN, in "Structural Intermetallics," edited by M. V. Nathal *et al.* (TMS, 1997) p. 469.
11. C. T. LIU, *Scripta Metall.* **23** (1989) 875.
12. *Idem.*, *ibid.* **27** (1992) 599.

Received 10 April
and accepted 21 November 2001